OPTOELECTRONICS AND ADVANCED MATERIALS – RAPID COMMUNICATIONS Vol. 14, No. 11-12, November-December 2020, p. 509-514

A T-shaped printed planar antenna on epoxy-resin material for ISM/WiFi/Bluetooth/WiMAX/WLAN applications

REZAUL AZIM[a,*], KOLI DHAR[a], MD MOTTAHIR ALAM[b], M. TARIQUL ISLAM[c]
[a]*Department of Physics, University of Chittagong, Chittagong 4331, Bangladesh*
[b]*Department of Electrical and Computer Engineering, King Abdulaziz University, Jeddah 21589, Saudi Arabia*
[c]*Department of Electrical, Electronic & Systems Engineering, Faculty of Engineering & Built Environment, Universiti Kebangsaan Malaysia(UKM), 43600 Bangi, Malaysia*

This paper presents a printed planar antenna for numerous wireless communication applications. The antenna is comprised of a T-shaped patch and partial ground plane and fabricated on epoxy-resin material. The antenna achieved a good operating bandwidth of 1.54 GHz ranging from 2.02 to 3.56 GHz (55.2 %), an average gain of 3.09 dBi, and average efficiency of 85 %. The measured results matched quite well to the simulated one and revealed that the studied antenna is able to satisfy the bandwidth and gain requirements with stable radiation patterns for different wireless commutation services including WiFi, ISM band, Bluetooth, WiMAX and WLAN.

(Received April 20, 2020; accepted November 25, 2020)

Keywords: Antenna, Bluetooth, ISM band, WiFi, wideband, WiMAX, WLAN

1. Introduction

The proliferation of wireless communications has entered into a new era of wireless networking. Wireless local area networks (WLANs) and cellular phones are undoubtedly the most popular wireless systems, but in the recent years, there has been substantial growth in the use of industrial, scientific and medical (ISM) frequency bands. According to the code of federal regulations of the FCC [1] and ITU regulations [2], the ISM bands are for the operation of 'equipment of appliances designed to generate and use locally RF energy for industrial, scientific, medical, domestic of similar purposes'. FCC allocates a number of frequency bands for ISM applications and commonly used bands are 433.05 – 434.79 MHz, 902 – 928 MHz, 2.4 – 2.5 GHz, 5.725 – 5.875 GHz [3]. Typical applications of ISM bands are the production of physical, biological, or chemical effects such as heating, ionization of gases, mechanical vibrations, hair removal and acceleration of charged particles. At the same time use of ISM frequency band in WiFi, Bluetooth, WiMAX, Zigbee, wireless telephones, are ongoing. WLANs under IEEE 802.11b standard [4], is another most widespread standards that use the 2.45 GHz ISM band for signal transception. Among different frequency bands, the 2.45 GHz ISM band is the most widely used band that lessens the system size.

Antenna plays a key role in transmitting and receiving of signal in any wireless communication. In ISM band applications, antennas should be small enough to be implanted in the human body. At the same time, they should have to be planar profile to be integrated in portable devices. Since the ISM antenna operates with the other wireless standard such as WiFi (2.4 GHz), Bluetooth (2.45 GHz), WiMAX (2.3, 2.5, 3.5 GHz) and WLAN (2.45 GHz), a wideband/multiband antenna that can cover all these narrow-band services is therefore necessary.

Different techniques and attempt have been reported to design wideband planar antennas [5-18]. For example, a metamaterial inspired triple-band antenna was reported in [5]. The resonant modes at 2.4 GHz, 3.5 GHz and 5 GHz were achieved by using a rectangular slot and a metamaterial inspired split ring structure. In [6], a planar antenna was reported to operate at 2.4 GHz and 3.5 GHz bands. To resonate at 2.4 GHz it uses microstrip line loaded with dumbbell-shape defected structure while the higher resonance was achieved by the use of two vias. In [7], a textile PIFA antenna was presented for ISM band applications. By embedding slots both in the patch and ground plane, the designed antenna was attained dual operating bands centred at 433 MHz and 2.4 GHz. However, the antenna possesses a large size of 140 × 80 mm^2. A built-in monopole inverted-F antenna for GPS and ISM operations was reported in [8]. For medical implant communication service (MICS) and ISM band applications, a dual-band stacked patch antenna was presented in [9]. The antenna consists of a two-stacked patch over a circular ground plane. The upper and lower patches resonate in MICS and ISM bands, respectively. However, it has a larger 3D profile and not suitable to be integrated into portable devices. In [10], a chip-type antenna that uses advanced meander line technique was presented for ISM band applications. The antenna is composed of small

ceramic dielectric and TMM-4 substrate and is able operates at 2.4 - 2.4835 GHz and 5.725 - 5.85 GHz bands. For WLAN application, a dual-band antenna was presented in [11]. This design adopts microstrip feedline, folded T-shaped radiator and two symmetrical rectangular patches and able to operate at dual frequency bands of 2.4 - 2.52 GHz and 4.5 - 7.5 GHz. A loop antenna with a band-stop matching circuit was developed in [12]. With a volumetric size of 14 × 55 × 0.8 mm^3, the designed antenna is able to operate at two wide operating bands of 704 - 960 MHz and 1710 - 2690 MHz. In [13], a multi-band planar antenna was reported to operate over the 900 MHz GSM band, the 2.45 GHz ISM band, and the 3.5/5 GHz WLAN band. A double band antenna operates over the LTE band was proposed in [14]. The studied antenna consists of L-shaped branch and meander lines and able to operate at 870 - 990 MHz (GSM band) and 1.65 - 3.14 GHz bands. In [15], a U-shaped open-end slot antenna was developed for handset applications. With a volumetric size of 12 × 58 × 0.6 mm^3, the designed antenna is able to operate in LTE band 12, DCS, PCS, UMTS, LTE band 40, ISM 2.45 GHz, LTE Band 42 and LTE band 43. Despite the attainment of wide/multiple operating bands, most of the above-mentioned antennas possess complex structure, larger dimension, 3D profile, low gain and low efficiency, which require more investigation to get an appropriate wideband antenna solution.

In this paper, a microstrip planar antenna is studied for WiFi/ISM band/Bluetooth/WiMAX/WLAN applications. The studied antenna has a simple structure and is prototyped on a low-cost epoxy-resin substrate material. It is revealed from the experimental observation that the presented antenna has an operating band of 2.02 - 3.56 GHz and able to cover the above mentioned multiple wireless services.

2. Antenna design and optimization

The design of the studied antenna starts with the basic equations for calculating the width (W) and length (L) of the microstrip patch antenna using the transmission line model. According to the transmission line model, the width, W and length, L of the rectangular patch are [19]

$$W = \frac{c}{2 f_0 \sqrt{\frac{\varepsilon_r + 1}{2}}} \tag{1}$$

and

$$L = \frac{c}{2 f_0 \sqrt{\varepsilon_e}} - 2\Lambda l \tag{2}$$

where f_o is resonance frequency, c is the speed of light in vacuum and ε_r is the relative permittivity. The effective permittivity is given approximately by [20]

$$\varepsilon_e = \frac{\varepsilon_r + 1}{2} + \frac{\varepsilon_r + 1}{2}\left[1 + \frac{12h}{W}\right]^{-\frac{1}{2}} \tag{3}$$

where h is the height of the dielectric substrate.

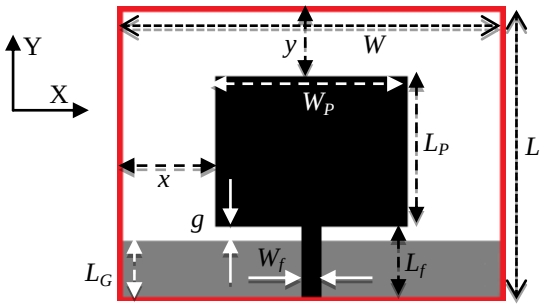

Fig. 1. Footprint of the proposed antenna

The antenna looks electrically larger than its physical dimensions due to the adjoining field around the boundary of the patch [20]. Considering this result Δl, the extension of length due to the fringing field effect is

$$\Lambda l = 0.412h \frac{\left(\varepsilon_e + 0.3\right)\left(\frac{W}{h} + 0.264\right)}{\left(\varepsilon_e - 0.258\right)\left(\frac{W}{h} + 0.8\right)} \tag{4}$$

The footprint of the studied antenna is displayed in Fig. 1. It comprised of a rectangular patch and a partial ground plane. The radiation element of dimensions W_P × L_P is printed on the front side of 1.6 mm-high epoxy-resin substrate material (FR4) with relative permittivity 4.6 and dielectric loss of 0.02. Despite slightly higher loss tangent, FR4 material is chosen for this design due to its low fabrication cost for mass production. A microstrip line of size W_f × L_f is also etched on the front side of the substrate to feed the antenna. The characteristics impedance of the feedline is fixed at 50 Ω. A ground plane of side length L_G is etched on the backside of the substrate. The optimized design parameters of the studied antenna are as follows: W = 79.8 mm, L = 57.8 mm, W_P = 38 mm, L_P = 29.4 mm, W_f = 3.1 mm, L_f = 14.2 mm, L_G= 12.74 mm, g = 1.46 mm x = 20.9 mm, and y = 14.2 mm.

The radiation mechanism of the antenna can properly understand by investigating the current distributions rather than input impedance characteristics that only describe the behaviour of the antenna as a lumped element at the end of microstrip feedline. The surface current distributions of the studied antenna at the first resonance frequency of 2.49 GHz is shown in Fig. 2(a) where the red colour indicates the strongest current while the blue colour is the weakest one. At this frequency, the surface current is mostly concentrated on the edge of the patch, ground plane and lower end of the feedline that implies that the fundamental

resonance mode is associated with patch and ground plane. At 3.2 GHz, shown in Fig. 2(b), the strongest current is confined in the gap between patch and ground plane and in the feedline which can be considered as the higher-order mode of 2.49 GHz. The current distributions in Fig. 2 confirmed that the radiating patch matched well with the partial ground plane results in the exhibition of wide impedance band.

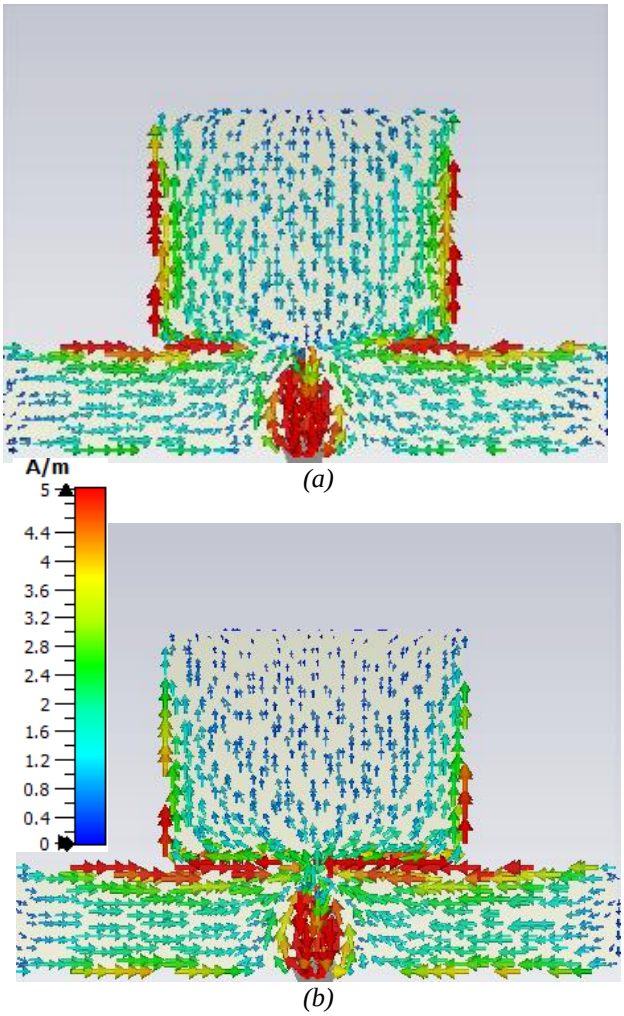

Fig. 2. Surface current distribution at (a) 2.49 GHz, and (b) 3.2 GHz (color online)

3. Results and discussion

To design the proposed wideband band antenna, a comprehensive parametric study has been conducted which helped to understand the effect of different parameters on antenna performances. The ground plane length, L_G is the first parameter to be optimized. In many open literatures, the strong dependence of the operating band of microstrip patch antenna on ground plane size has been reported [21-22]. The variation of simulated S_{11} for different values of L_G is displayed in Fig. 3(a), which indicated that decreasing and increasing of L_G from its final value demonstrates poor operating band with worst S_{11}. In this design a value of L_G = 12.74 mm is optimized to exhibits widest bandwidth with best S_{11} value of -35.72 dB at 2.49 GHz. The simulated S_{11} for different values of feedline width, W_f is shown in Fig. 3(b). As the W_f adjusts the 50 Ω characteristics impedance of the feedline, it can tune the operating band of the studied antenna. It can be observed from the plot that a width of 3.1 mm can offer the required operating band with best S_{11} value. Fig. 3(c) demonstrates the simulated $S_{11}$with the different g, the gap between the patch and the ground plane, while the other parameters have remained unaltered.

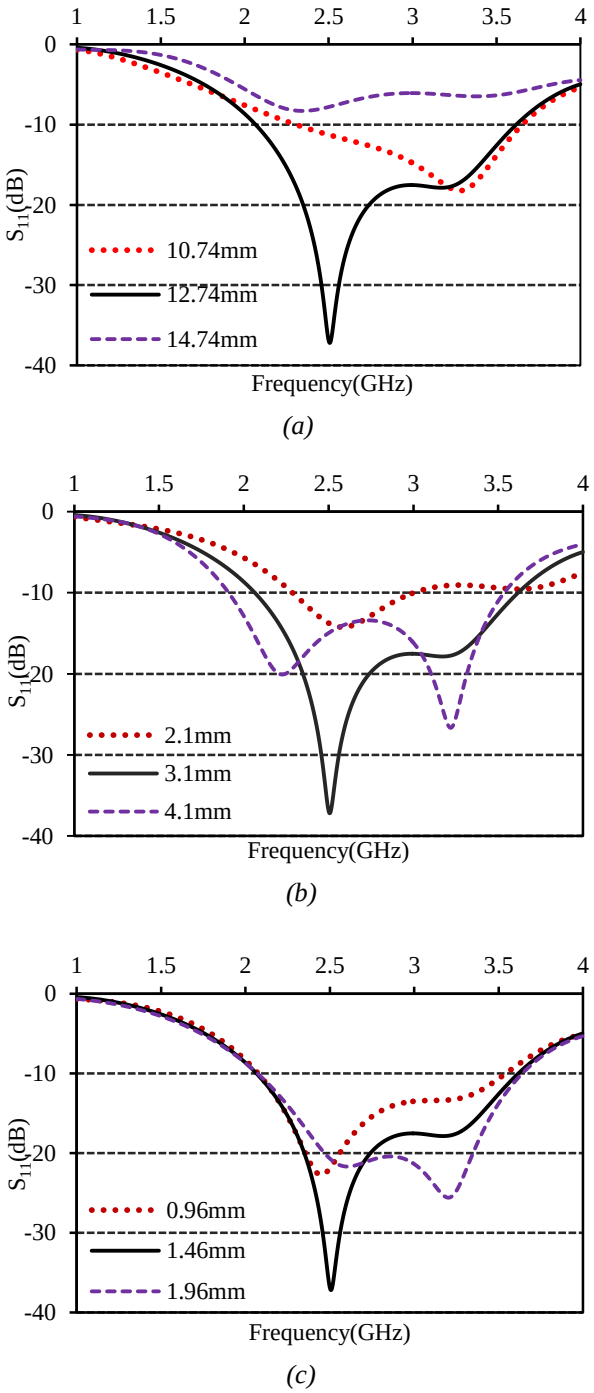

Fig. 3. Variation of S_{11} with (a) L_G, (b) W_f, and (c) g (color online)

As the ground plane act as an impedance matching circuit, the gap *g* can tune the input impedance of the antenna, results in a variation in the operating band. It can be seen from the plot that a gap of 1.46 mm can give a better S_{11} value within the required impedance bandwidth. The optimized structural parameters have been found after a comprehensive parametric study. A set of the prototype of the studied antenna has been fabricated using optimized parameters for experimental validation. The fabricated prototype of the proposed antenna is illustrated in Fig. 4. The S-parameter of the fabricated antenna has been measured using PNA N5227A Network Analyzer. The measured and simulated S_{11} responses of the proposed antenna are presented in Fig. 5. It is observed from the plot that the prototype antenna achieved an impedance bandwidth ranging from 2.02 – 3.56 GHz ($S_{11} \leq$ -10 dB) which covers the 2.45 GHz ISM band as well as WiFi 2.4 GHz, Bluetooth 2.45 GHz, WiMAX. 2.3 GHz, 2.5 GHz 3.5 GHz and WLAN 2.45 GHz. Slight discrepancies between the two results may be due to the effect of the RF feeding cable, which is used in the measurements but does not consider during the simulation.

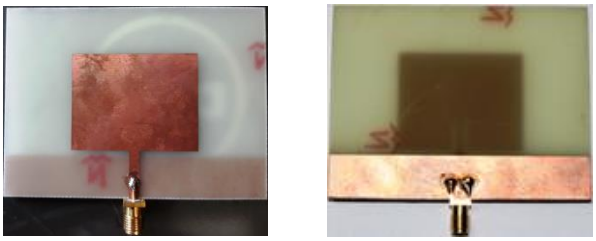

Fig. 4. Prototype of the designed antenna (color online)

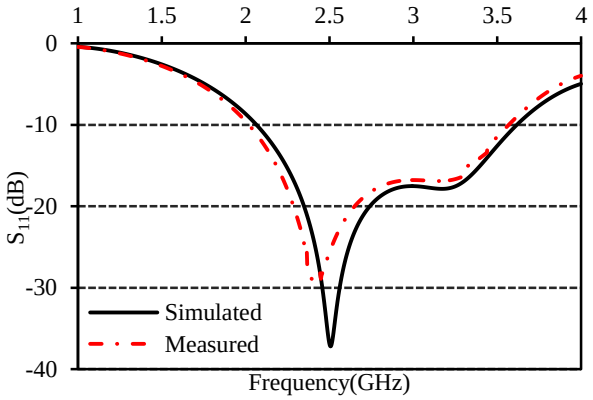

Fig. 5. Simulated and measured S_{11} responses of the proposed antenna (color online)

The gain, efficiency and radiation patterns of the studied antenna are measured using the StarLab near-field measurement system as shown in Fig. 6 [23]. The measured peak gain of the studied antenna is shown in Fig. 7 from where it can be observed that the designed antenna achieved an average gain of 3.09 dBi with a maximum of 3.84 dBi. The radiation efficiency of the studied antenna presented in Fig. 8 displays that average measured radiation efficiency in the operating band is 84.66 % with a maximum efficiency of 92.38 %. The gain and efficiency of the proposed antenna can be improved using a more expensive microwave substrate rather than standard low-cost epoxy-resin material.

The radiation patterns of the proposed antenna in *E*-plane and *H*-plane planes are measured at the resonance frequency of 2.49 GHz and 3.2 GHz. Fig. 9(a) demonstrates the 2D radiation patterns at 2.45 GHz in terms of co-polarized field (E_θ) and cross-polarized filed (E_ϕ) components while Fig. 9(b) present the patterns at 3.2 GHz. It can be observed from the plot that at both frequencies the designed antenna exhibits typical dipole like radiation characteristics.

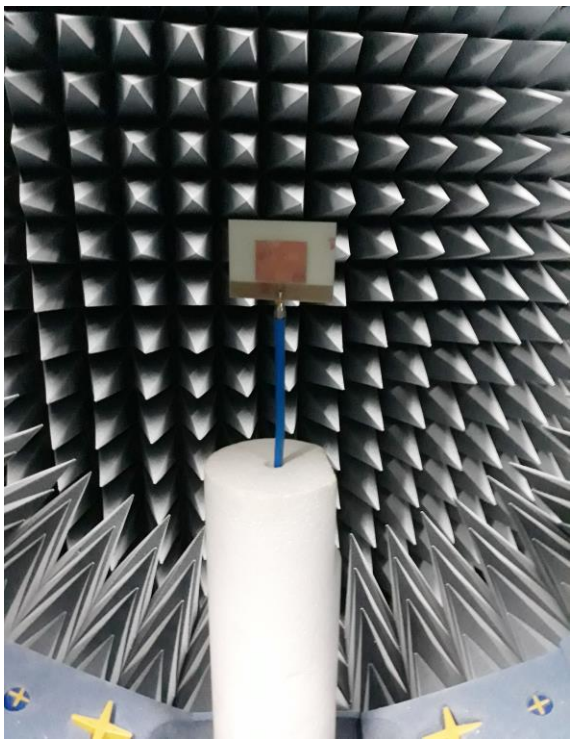

Fig. 6. Radiation Characteristics measurement set-up in StarLab

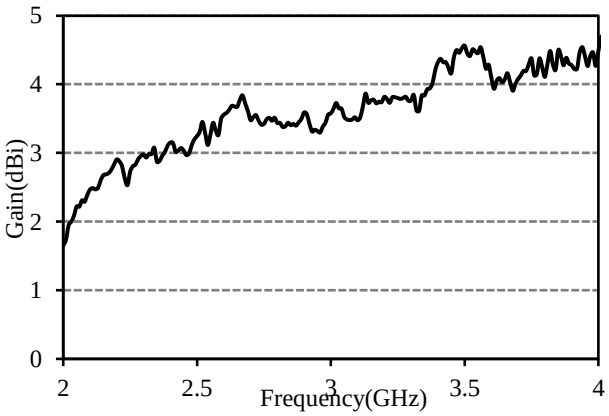

Fig. 7. Measured peak gain of the proposed antenna

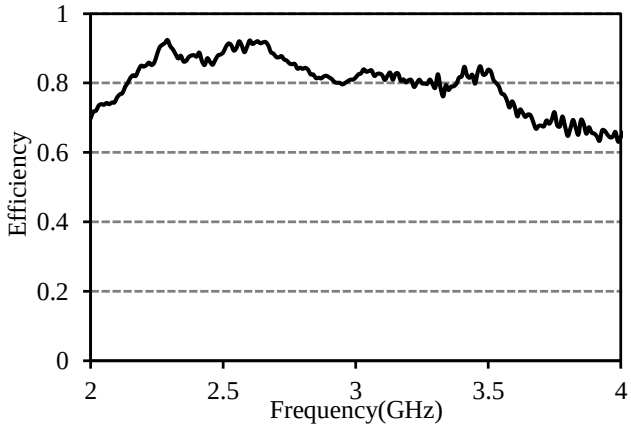

Fig. 8. Measured efficiency of the proposed antenna

The simulated three-dimensional radiation pattern for the total electric field (*E*) at 2.49 GHz is shown in Fig. 10. In the pattern, the red colour indicates the strongest radiated *E*-field while the blue colour is the weakest one. From the 3D pattern, it is also revealed that the radiation pattern is dipole like with nulls in bore-site directions. Despite the nulls in the bore-site directions, the radiation patterns of the studied antenna are symmetric over the entire working band, which is a prime requisite for many narrow-band wireless communication applications.

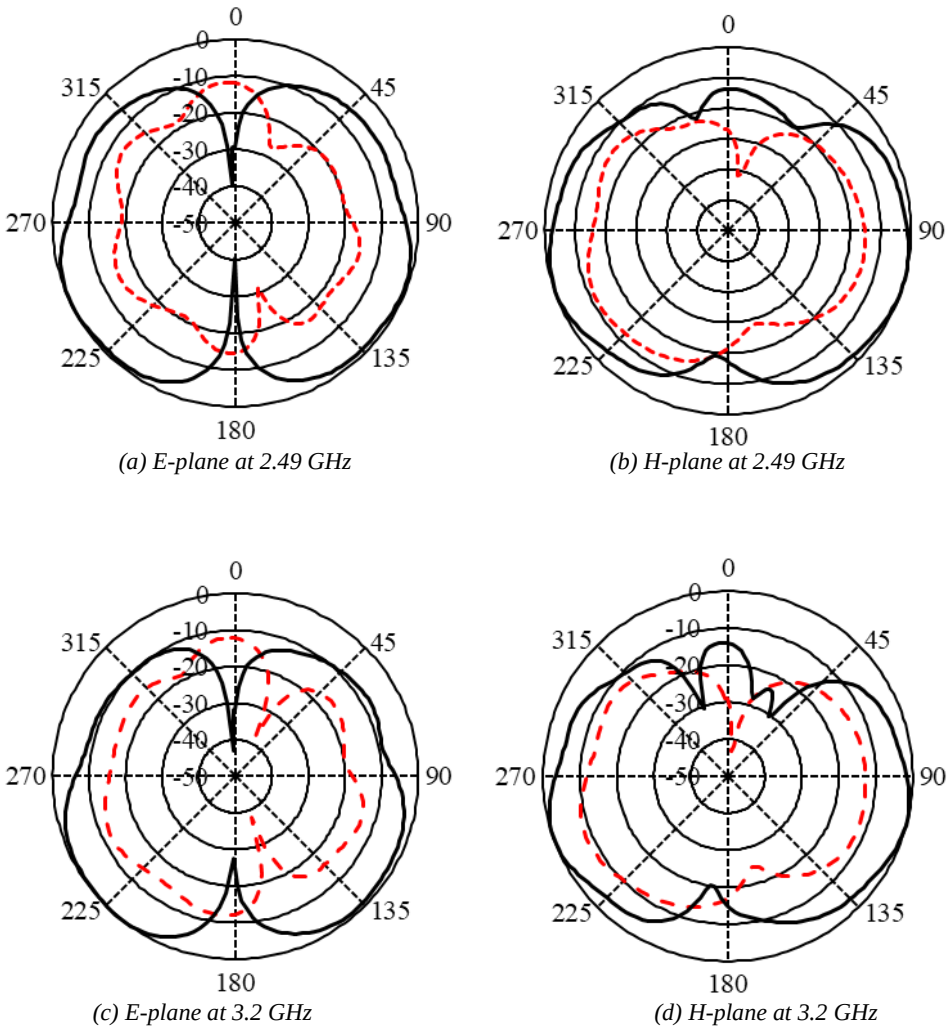

(a) E-plane at 2.49 GHz

(b) H-plane at 2.49 GHz

(c) E-plane at 3.2 GHz

(d) H-plane at 3.2 GHz

Fig. 9. Measured radiation patterns at different frequencies. In the plot, the solid black lines represent the co-polarized components (E_θ) while the dotted red lines represent the cross-polarized components (E_ϕ) (color online)

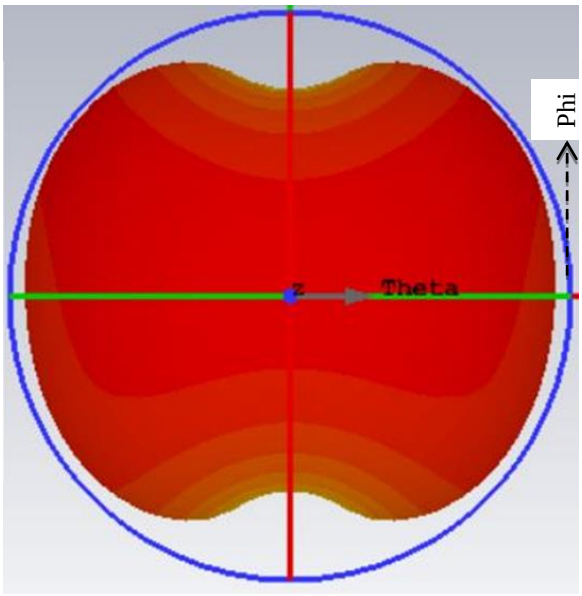

Fig. 10. Simulated 3D radiation pattern at 2.49 GHz (color online)

4. Conclusions

In this paper, a low-profile T-shaped microstrip planar antenna is presented. The studied antenna consists of a T-shaped patch and a small ground plane and fabricated on both sides of an epoxy-resin microwave substrate material. Experimental and theoretical results demonstrate that the radiating element coupled well with the ground plane and the presented antenna able to achieve an operating band of 1.54 GHz (55.2 %) covering WiFi (2.4 GHz), ISM band (2.45 GHz), Bluetooth (2.45 GHz), WiMAX (2.3 GHz, 2.5 GHz, and 3.5 GHz) and WLAN (2.45 GHz). The designed antenna also has a good gain, efficiency and demonstrates stable radiation patterns that make it a good candidate to be used in numerous wireless communication applications.

Acknowledgements

This work is financially supported by the Ministry of Higher Education, Malaysia having the fundamental research grant number FRGS/1/2014/TK03/UKM/01/1.

References

[1] "Federal Communications Commission (FCC)," http://www.fcc.gov.
[2] "International Telecommunication Union," https://www.itu.int/en/Pages/default.aspx.
[3] "Part 18: Industrial, Scientific and Medical Equipment," FCC Rules and Regulations **1**, 877.
[4] "IEEE Standard Association," http://standards.ieee.org
[5] V. Rajeshkumar, S. A. Raghavan, Int. J. Electron. Commun. **69**(1), 274 (2015).
[6] J. Malik, A. Patnaik, M. V. Kartikeyan, IEEE Antennas Wirel. Propag. Lett. **14**, 503 (2015).
[7] S. Yan, V. Volskiy, G. A. E. Vandenbosch, IEEE Antennas Wirel. Propag. Lett. **16**, 2436 (2017).
[8] M.-A. Chung, C.-F. Yang, IET Microw. Antennas Propag. **10**(12), 1285 (2016).
[9] S. Chamaani, A. Akbarpour, IEEE Antennas Wirel. Propag. Lett. **14**, 1722 (2015).
[10] J.-I. Moon, S.-O. Park, IEEE Antennas Wirel. Propag. Lett. **2**, 313 (2003).
[11] J. Yang, H. Wang, Z. Lv, H. Wang, Sensors **16**, 1 (2016).
[12] K.-L. Wong, T.-J. Wu, Microw. Opt. Technol. Lett. **54**(5), 1189 (2012).
[13] H. J. Liu, R. L. Li, Y. Pan, X. L. Quan, L. Yang, L. Zheng, IEEE Trans. Antennas Propag. **62**(5) 2856 (2014).
[14] V. Ghaffari, A. Tavakkoli, R. M. Boroujeni, Proc. ICEE 2016, Shiraz, Iran, 2016, pp. 1244-1247.
[15] C.-K. Hsu, S.-J. Chung, IEEE Trans. Antennas Propag. **62**(2), 929 (2014).
[16] M. Samsuzzaman, T. Islam, N. A. Rahman, M. R. I. Faruque, J. Mandeep, Int. J. Antennas Propag. **2014**, 1 (2014).
[17] M. Samsuzzaman, M. Mahmud, M. T. Islam, M. Ali, M. T. Islam, Microwave Opt. Technol. Lett. **59**(7), 1590 (2017).
[18] R. Azim, M. T. Islam, Mater. Tehnol. **49**(2), 193 (2015).
[19] J. P. Gilb, C. A. Balanis, IEEE Trans. Microw. Theory Tech. **37**, 1620 (1989).
[20] P. Bhartia, I. Bahl, R. Garg, A. Ittipiboon, "Microstrip Antenna Design Handbook", Artech House Publishers, Norwood, Massachusetts, USA, 2000.
[21] R. Azim, M. T. Islam, N. Misran, Appl. Comput. Electromagn. Soc. J. **26**(10), 856 (2011).
[22] R. Azim, M. T. Islam, N. Misran, Arab. J. Sci. Eng. **38**(9), 2415 (2013).
[23] Microwave Vision Group, StarLab, https://www.microwavevision.com.

*Corresponding author: rezaulazim@cu.ac.bd